ISSN 0023-1584, Kinetics and Catalysis, 2006, Vol. 47, No. 3, pp. 445–450. © MAIK "Nauka/Interperiodica" (Russia), 2006.
Original Russian Text © V.V. Chesnokov, R.A. Buyanov, I.V. Mishakov, V.I. Zaikovskii, 2006, published in Kinetika i Kataliz, 2006, Vol. 47, No. 3, pp. 454–460.

Effect of Zinc Added to the Co/Al_2O_3 Catalyst on the Formation of Carbon Nanofilaments from Methane and Butadiene-1,3

V. V. Chesnokov, R. A. Buyanov, I. V. Mishakov, and V. I. Zaikovskii

Boreskov Institute of Catalysis, Siberian Division, Russian Academy of Sciences, Novosibirsk, 630090 Russia
e-mail: chesn@catalysis.ru

Received October 15, 2004

Abstract—The dynamics of carbon nanofilament growth from methane and butadiene-1,3 on $Co–Zn/Al_2O_3$ catalysts have been studied in the temperature range 500–750°C. The rate-limiting step in the growth of nanofilaments from butadiene is carbon atom diffusion through the bulk of the metal particle. In the case of methane, the process is controlled by one of the stages of hydrocarbon decomposition on the metal particle. The structure and morphology of the nanofilaments (composites) forming by the carbide cycle mechanism on fine zinc-promoted cobalt particles have been studied by electron microscopy and X-ray diffraction. The morphology and crystallographic properties of the nanofilaments depend on the ratio of the hydrocarbon decomposition rate (which is determined by the nature of the hydrocarbon) to the rate at which carbon atoms diffuse from their formation sites to the nanofilament formation sites (which is determined by the nature of the metal particle and by the carbon diffusion coefficient in the particle bulk). The properties of the resulting carbon nanofilaments can be controlled by varying the nature of the hydrocarbon to be decomposed and the reaction temperature and by introducing another metal into the cobalt particles.

DOI: 10.1134/S0023158406030177

In the last 20–30 years, there have been hundreds of publications devoted to the methods and laws of the synthesis of various carbon composites important to practice. Technologies based on various formation mechanisms have been suggested for obtaining these materials [1].

The decomposition of hydrocarbons on fine particles of iron-family metals and their alloys with other metals via the carbide cycle mechanism yields carbon phases varying in morphology and crystallographic features [2–4]. In most cases, these phases form nanofilaments; in certain cases, they form other, more complex structures.

In an earlier work [4], we considered two main stages of the formation of the carbon phases. The chemical stage includes the catalytic decomposition of the hydrocarbon into carbon atoms on the "frontal side" of a fine metal particle and the growth of carbon concentration in the particle bulk up to saturation. The physical stage includes graphite nucleation on the backside of the particle, the diffusion of forming carbon atoms to the nucleation centers, and, as a consequence, the growth of the graphite phase. The morphology and crystallographic properties of the resulting carbon phase are mainly determined by second-stage conditions and processes.

The metal particles on the ends of growing carbon nanofilaments change their faceting and shape. When the carbon growth rate is high, elongated metal particles are observed in nanofilament channels.

It follows from the totality of previous data [4] that the properties of the resulting carbon phase are governed by the properties of the metal particle at the second stage of the carbide cycle. The problem is learning to control the properties of the metal particle and, thereby, the formation of the carbon composite. The most promising way of doing this is by adding another metal to the iron-family metal particle in order to change many of its properties and its behavior.

In a recent review [4], we considered the stepped mechanism of carbon nanofilament and nanotube formation. However, understanding only the general principles of this process is insufficient for controlling it. It is equally important to know its specific features arising from the nature and composition of the fine metal particles. Elucidating these specific features would provide a deeper and, possibly, much more correct insight into the general principles. A theory that ignores or cannot explain specific features is not comprehensive and has no predictive force.

This work is concerned with cobalt, an iron family metal that has received the least investigation. To facilitate the transformation of alloy particles, the cobalt catalyst was modified with zinc (M), a low-melting metal. The formation of carbon nanofilaments on Co–M bimetallic catalysts is poorly understood, and there is no information concerning Co–Zn catalysts.

The modifying effect of the second component was demonstrated by adding small amounts of silver to cobalt [5]. Adding 1% Ag to the Co catalyst increased,

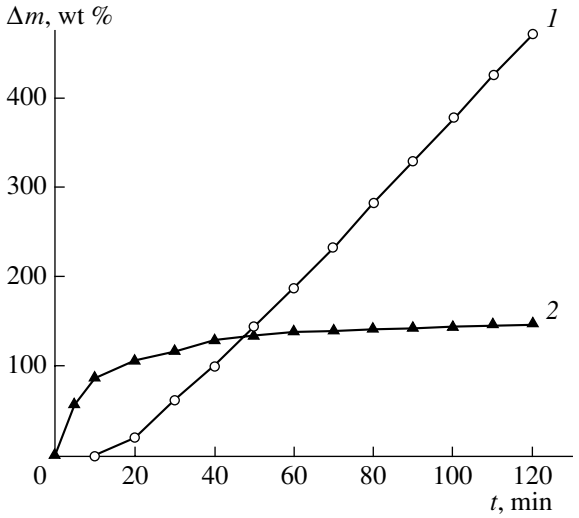

Fig. 1. Dynamics of carbon formation from (*1*) methane and (*2*) argon-diluted butadiene-1,3 (C_4H_6 : Ar = 1 : 75) on the Co/Al_2O_3 catalyst at 500°C.

by one order of magnitude, the yield of filamentous carbon resulting from the decomposition of ethylene at 600°C. Unfortunately, no convincing explanation has been suggested for this effect.

The metals in the Co–Cu system interact strongly [6, 7], although, according to the phase diagram, copper is negligibly soluble in cobalt. Furthermore, copper changes the morphology of filamentous carbon: the ordinary, straight-line nanofilaments are replaced with carbon deposits called octopuses, in which one cobalt–copper particle initiates the growth of several filaments in different directions. For the first time, this morphology was observed with nickel–copper alloys [8–11].

There has been a study [12] of the synthesis of one-walled carbon nanotubes in the presence of cobalt modified with Sn, Pd, Ru, Fe, Ni, W, and Pt. The yield of nanotubes is reduced by Sn, Ru, Fe, and Pd and is affected only slightly by W and Ni. The highest yield of one-walled nanotubes was observed with Co–Pt catalysts. These findings are purely empirical and provide no insight into the mechanism of the modifying effect.

Here, we report the effect of zinc in Co–Zn bimetallic particles on the formation of carbon nanofilaments from methane and butadiene-1,3.

EXPERIMENTAL

$Co–Zn/Al_2O_3$ catalysts containing 10 wt % Al_2O_3 and 90 wt % (Co + Zn) were prepared by coprecipitation from aqueous cobalt and aluminum nitrate and zinc acetate solutions at pH 9.5. The Co/Zn atomic ratio was 32.3, 9.0, 4.0, or 1.0.

The coprecipitated catalysts were dried at 120°C and were then heat-treated in air at 330°C. Prior to the experiments, the catalysts were heated in flowing hydrogen to 550°C within 20–30 min. Before being brought into contact with air, the reduced cobalt-containing catalysts were passivated in an argon flow (80 l/h) into which oxygen (3 l/h) was introduced as 0.5- to 1.0-min-long pulses.

The formation of carbon from methane and butadiene-1,3 was studied in a quartz flow reactor with a McBain balance under zero-gradient thermal conditions [13]. The sample weight was 0.01–0.05 g. The sensitivity of the weight-measuring system was 1×10^{-4} g. Weight gain was calculated using the formula $\Delta m = (m(t) - m(0))/m_0 \times 100\%$.

Methane was 99.92 vol % pure, butadiene was 98 vol % pure (the balance being butenes), and argon was 99.7 vol % pure.

X-ray diffraction patterns were obtained on a D-500 diffractometer (Siemens) using monochromated CuK_α radiation (graphite monochromator in the reflected beam).

Carbonized catalysts were examined by transmission electron microscopy (JEM-100CX microscope; accelerating voltage, 100 kV; spherical aberration coefficient of the objective lens, 2.8 mm; line resolution capacity, 2 Å). Carbon structures were carefully examined by high-resolution electron microscopy in combination with electron diffraction (JEM-2010 instrument; line resolution, 1.4 Å).

RESULTS AND DISCUSSION

Alumina–Cobalt Catalysts

After calcination at 330°C, the catalysts were solid solutions of aluminum in Co_3O_4 with a coherent-scattering region of 80 Å. During reduction at 550°C, this solid solution separated to yield fine particles of cobalt metal with a coherent-scattering region of 120 Å. In cobalt-rich alumina–cobalt catalysts, alumina stabilizes the finely dispersed cobalt metal that results from hydrogen treatment. Nevertheless, the coherent-scattering region grows upon the reduction of the sample because of the partial sintering of Co. No reflections assignable to alumina were observed in the diffraction patterns.

Numerous stacking faults were observed in the cobalt metal particles that resulted from the reduction of the alumina–cobalt catalysts. These faults were most likely to be due to cobalt having a microdomain structure with alternating cubic and hexagonal coherent domains.

The formation of morphologically different carbon structures from methane and butadiene-1,3 was studied for the 90 wt % Co/Al_2O_3 catalyst.

Methane and butadiene-1,3 differ in terms of carbon formation dynamics on the Co/Al_2O_3 catalyst (Fig. 1). It is well known that most information is provided by the initial kinetics, which characterize the process rate not slowed down by reaction products. In the formation of carbon from methane, there is an induction period

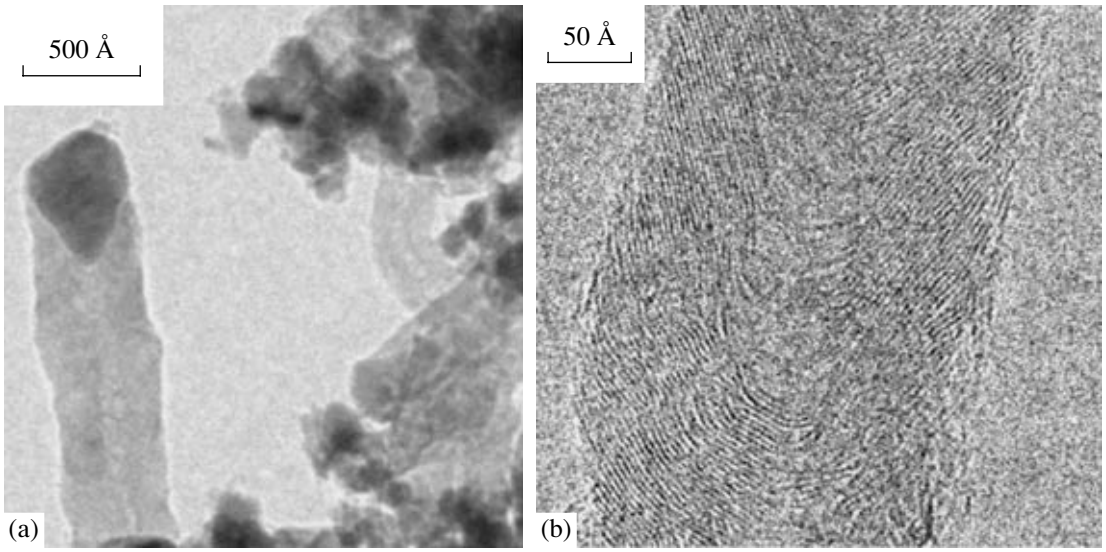

Fig. 2. Electron micrographs of carbon nanofilaments obtained from methane on the Co/Al_2O_3 catalyst at 500°C: (a) morphology and (b) structure.

followed by a marked increase in the reaction rate. As a whole, the initial stage of carbon formation on the Co/Al_2O_3 catalyst is slower for methane than for butadiene-1,3. This is due to the fact that these hydrocarbons differ in stability and decomposition rate. In view of this, the hydrocarbons are apparently different in terms of the rate-limiting step of carbon formation.

At 500–750°C, the rate-limiting step in the formation of carbon nanofilaments from unsaturated hydrocarbons (butadiene-1,3 and acetylene) is the diffusion of carbon atoms to graphite nuclei through the metal bulk [4], as is indicated by the facts that the order of the reaction with respect to butadiene is zero and the activation energy is 38 kcal/mol. In this case, the formation of carbon atoms on the frontal side of a metal particle is more rapid than the removal of these atoms by diffusion transport to the backside of the particle. As a consequence, the frontal side of the particle is coated with excess carbon and the process is almost terminated (Fig. 1, curve *2*).

In the case of methane, the rate-limiting step is apparently graphite nucleation at the early stages of the reaction, which is followed by methane decomposition on the cobalt metal surface. At the latter stage, the carbon deposition rate increases to reach its steady-state value. The activation energy was determined from the temperature dependence of the steady-state rate to be 12 kcal/mol. This value is thrice lower than the activation energy of carbon diffusion through cobalt bulk.

Differing in terms of carbon formation kinetics, methane and butadiene-1,3 afford carbon nanofilaments with different morphologies. The nanofilaments obtained from methane have the structure of stacked coaxial cones (Fig. 2).

By contrast, the decomposition of butadiene-1,3 yields coaxial cylindrical nanotubes throughout the temperature range 500–750°C (Fig. 3). The diameter of these nanotubes is equal to the diameter of cobalt particles determined by X-ray diffraction. The nanotube diameter was 60 to 150 Å at 500°C and 80 to 250 Å at 750°C. The diameter of the empty channel is smaller than the nanotube diameter by a factor of about 3. The number of carbon layers in a nanotube varies between

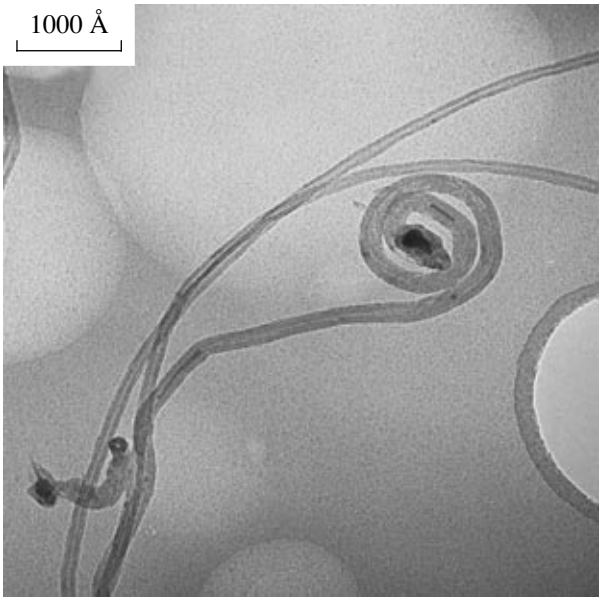

Fig. 3. Electron micrograph of a carbon nanotube obtained from a butadiene-1,3–argon (1 : 75 mol/mol) mixture on the Co/Al_2O_3 catalyst at 750°C.

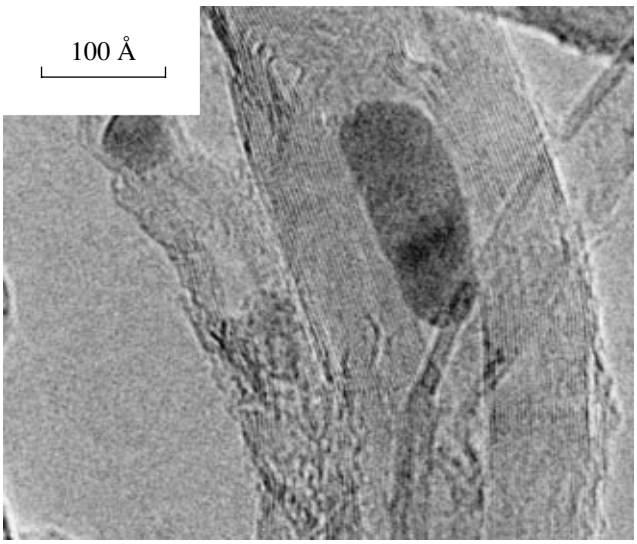

Fig. 4. Electron micrograph of a carbon nanotube containing a metal particle in its channel. $T = 750°C$.

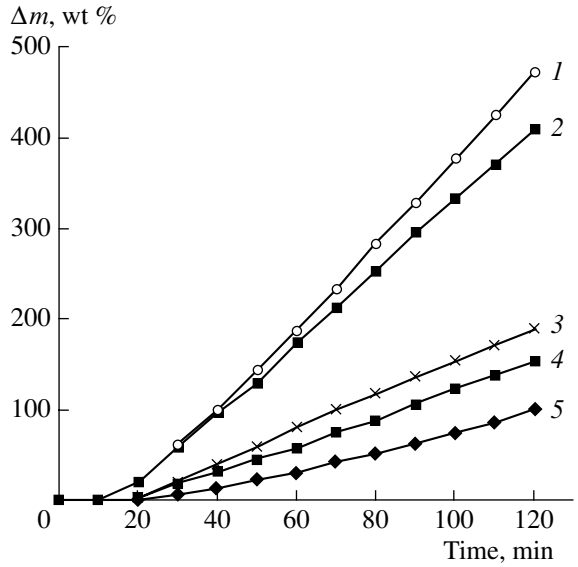

Fig. 5. Dynamics of carbon formation from methane at 500°C on the Co–Zn/Al_2O_3 catalysts. Zn content: (*1*) 0, (*2*) 3, (*3*) 10, (*4*) 20, and (*5*) 50 wt %.

6 and 25. Some nanotubes contain metal particles in their channel (Fig. 4).

Therefore, the formation of carbon phases by the carbide cycle mechanism depends on the hydrocarbon decomposed. Apparently, the morphology and crystal structure of carbon composites depend on the ratio of the hydrocarbon decomposition rate on the frontal side of the metal particle and the rate of carbon atom diffusion to the backside of the particle. In turn, this ratio depends not only on the hydrocarbon but also on the carbon diffusion coefficient in the bulk of the particle, whose properties can be modified by adding various metals.

Cobalt–Zinc System (Co–Zn/Al_2O_3)

We examined systems containing 3, 10, 20, and 50% Zn relative to Co. The catalysts with >50% Zn show a much lower activity in the formation of carbon nanofilaments, and it was of no interest to characterize them by physicochemical methods. After precipitation and calcination at 330°C, only a Co_3O_4-based solid solution was identified by X-ray diffraction in the specimens containing 3, 10, and 20% Zn and the specimen containing 50 wt % Zn was amorphous to X-rays. After hydrogen reduction at 550°C, the Co and CoO phases were identified in the 3, 10, and 20% Zn specimens and the same phases and ZnO were identified in the 50 wt % Zn specimen. The presence of CoO is explained by the oxidation of cobalt metal upon the passivation of the catalyst with oxygen at room temperature. The size of a coherent-scattering region in the cobalt particles is 120 Å for the 3–10% Zn specimens and 90 Å for the 50% Zn specimen.

Carbonization of the Co–Zn/Al_2O_3 Catalysts in Methane

The rate of carbon formation from methane decreases as the zinc content of Co–Zn/Al_2O_3 is increased (Fig. 5). This is explained by both a decrease in the total Co content and a decrease in the Co concentration on the active surface of the bimetallic particle.

However, the slowdown in methane formation is not proportional to the decrease in the Co content because of the formation of solid solutions of zinc in cobalt. Indeed, as the zinc content is raised from 0 to 50%, the unit cell parameter of cobalt increases by 0.01 Å. This does not lead to any significant changes in the morphology of the carbon resulting from methane decomposition at 500°C. The carbon nanofilaments have a coaxial cone structure like that shown in Fig. 2.

According to the Co–Zn equilibrium diagram, the solubility of zinc in cobalt increases from 6 to 10 wt % as the temperature is raised from 500 to 600°C.

Raising the methane decomposition temperature to 600°C was expected to strengthen the interaction between zinc and cobalt. Indeed, examination of the catalysts carbonized at 600°C has demonstrated that zinc oxide undergoes extensive reduction at this temperature to yield a new Co–Zn compound.

Figure 6 shows the X-ray diffraction patterns from the Co–Zn/Al_2O_3 catalysts coked to methane at 600°C. The phase composition of the specimen obtained under these conditions differs markedly from the phase composition of the Co–Zn/Al_2O_3 catalysts obtained at 500°C. Apparently, a solid solution of zinc in cobalt forms at a low zinc content (3–10%). At a zinc content of 20–50%, zinc metal reacts with cobalt to yield a cubic cobalt–zinc compound (space group *Pm*3*m*,

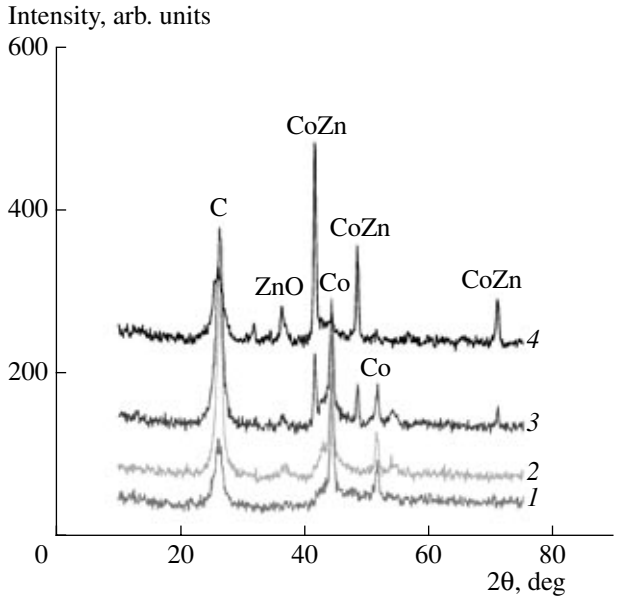

Fig. 6. X-ray diffraction patterns from $Co–Zn/Al_2O_3$ catalysts treated with methane at 600°C. Zn content: (*1*) 3, (*2*) 10, (*3*) 20, and (*4*) 50 wt %.

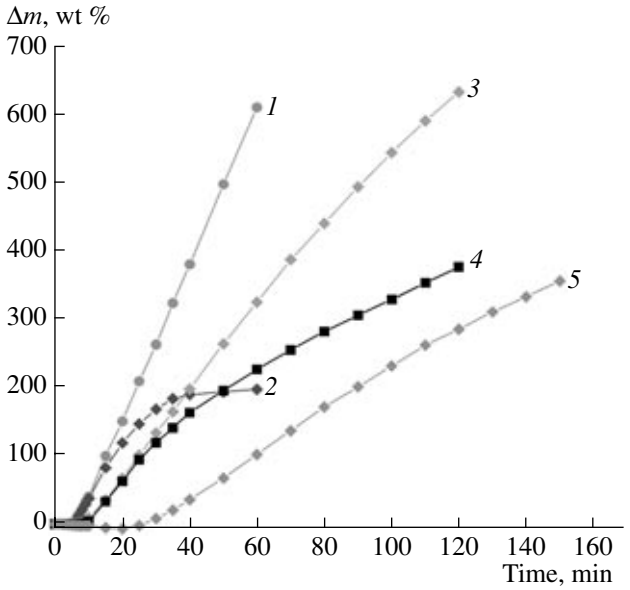

Fig. 7. Dynamics of carbon formation from methane at 600°C on the $CoZn/Al_2O_3$ catalysts. Zn content: (*1*) 0, (*2*) 3, (*3*) 10, (*4*) 20, and (*5*) 50 wt %.

a = 3.768 Å). As a consequence, as the zinc content is increased, the intensity of the α-Co lines decreases and the intensity of the reflections from the zinc–cobalt compound increases. The Powder Diffraction File contains no information concerning this compound. It is possible that this compound is a Co–Zn intermetallide or a Co–Zn carbide. The $Co–Zn/Al_2O_3$ catalyst treated with methane at 550°C has the same phase composition. Note that the hydrogen reduction of the $Co–Zn/Al_2O_3$ catalyst at 550°C does not yield a cobalt–zinc compound.

Note that the phase composition of the bimetallic particles forms during the growth of carbon filaments by the carbide cycle mechanism, when the particles are far from equilibrium. Therefore, in this case, the equilibrium phase diagrams cannot serve as a reference in the determination of the composition of these particles.

Such a particle is a dissipative system at dynamic equilibrium. The directed flow of carbon atoms acts to mix the components of the bimetallic particle, and a new Co–Zn compound forms under nonequilibrium conditions. The changes in the phase composition of the $Co–Zn/Al_2O_3$ catalyst affect both the carbon formation dynamics (Fig. 7) and the morphology of the resulting nanofilaments. The rate of carbon formation from methane decreases as the zinc content of the catalyst is increased. Therefore, the *Pm*3*m* cobalt–zinc compound shows a low activity in the formation of carbon nanofilaments.

The most interesting results were obtained with a low-zinc $Co–Zn/Al_2O_3$ catalyst. At the early stages of methane decomposition, adding 3 wt % Zn to the Co/Al_2O_3 catalysts exerts no effect on the nanofilament formation rate. However, this catalyst is rapidly deactivated during the reaction. This deactivation is explained by the fact that the small amount of zinc, a low-melting element, markedly lowers the melting point of the alloy particle without producing any significant effect on the methane decomposition rate or on the subsequent diffusion of carbon atoms through the bulk of the particle. The small zinc admixture and the intensive carbon atom diffusion through the particle bulk cause an additive decrease in the melting temperature of the alloy particle. This results in radical changes in the structure and morphology of the carbon nanofilaments. The coaxial cone structure observed for Co/Al_2O_3 is changed to a metal-filled nanotube structure. Even the addition of a small amount (3%) of zinc markedly affects the lability of the alloy particle occupying the nanotube channel.

Apparently, raising the zinc content of the zinc–cobalt alloy to ≥10% further decreases the melting point of the dissipative bimetallic system. As a consequence, the Co–Zn particles grow and aggregate into a sphere. However, increasing the zinc content of the catalyst reduces the diffusion flux of carbon atoms through the Co–Zn particle and, accordingly, raises the melting point. These changes in the properties of the Co–Zn particles cause changes in the structure and morphology of the resulting carbon nanofilaments. The carbon nanotubes filled with metal to a considerable extent are replaced with carbon nanofilaments with an octopus morphology such that several nanofilaments with a stacked structure grow out of one alloy particle (Fig. 8).

These changes in the nanofilament structure can be explained based on our understanding of graphite phase formation through hydrocarbon decomposition by the

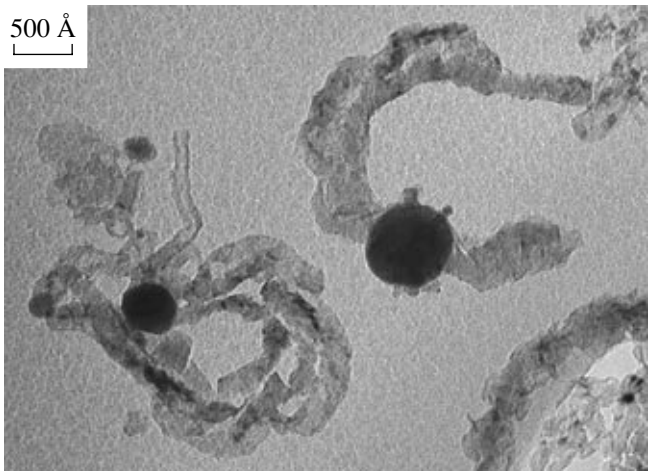

Fig. 8. Morphology of filamentous carbon obtained from methane on the (90% Co–10% Zn)/Al_2O_3 catalyst at 550°C.

carbide cycle mechanism. Apparently, the introduction of Zn into Co substantially decreases the carbon atom diffusion coefficient in the particle bulk. As a consequence, the carbon atoms in the Co–Zn particle diffuse to nearer (adjacent) faces, yielding nanofilaments with a stacked structure.

A Co–Zn compound inactive in carbon formation forms at a high zinc content of 20–50%. This is another cause of the fact that the catalytic activity falls as the zinc content of the catalyst is increased. The remainder Co–Zn alloy particles give rise to octopus-like carbon nanofilaments.

A more intensive carbon formation on the Co–Zn/Al_2O_3 catalysts is observed in the case of butadiene-1,3 diluted with argon to a molar ratio of 1 : 75. In this case, the Co–Zn compound decomposes partially to yield small Co particles, which then initiate the growth of coaxial cylindrical nanotubes. The carbon nanofilaments that form on the Co–Zn/Al_2O_3 catalysts at 500–750°C have the shape of a defective nanotube.

Thus, the actual dependences of the carbon nanofilament structure on the composition of the Co–Zn catalyst and on the methane and butadiene-1,3 decomposition temperatures appeared to be more complicated than was expected. This is due to the fact that this structure depends on of a number of variables characterizing the behavior of the dissipative bimetallic systems initiating the growth of carbon filaments by the carbide cycle mechanism.

The above results demonstrate, by the example of the Co–Zn/Al_2O_3 system, how the morphology and crystallographic properties of carbon composites can be controlled by varying the nature of the hydrocarbon to be decomposed and the carbon formation temperature and by introducing another metal into the fine iron-family metal particles.

ACKNOWLEDGMENTS

This work was supported by the Russian Foundation for Basic Research (project no. 03-03-32158), the Support to Leading Scientific Schools Program (grant no. NSh-5469.2006.3), and the Department of Chemistry and Materials Science of the Russian Academy of Sciences (grant no. 4.3.1).

REFERENCES

1. Mordkovich, V.Z., *Teor. Osn. Khim. Tekhnol.*, 2003, vol. 37, no. 5, p. 460.
2. Buyanov, R.A., Chesnokov, V.V., and Afanas'ev, A.D., *Izv. Sib. Otd. Akad. Nauk SSSR, Ser. Khim. Nauk*, 1981, vol. 4, no. 9, p. 28.
3. Buyanov, R.A., *Zakoksovanie katalizatorov* (Coking of Catalysts), Novosibirsk: Nauka, 1983.
4. Chesnokov, V.V. and Buyanov, R.A., *Usp. Khim.*, 2000, vol. 69, no. 7, p. 675.
5. Chambers, A., Rodriguez, N.M., and Baker, R.T.K., *J. Phys. Chem.*, 1996, vol. 100, no. 10, p. 4229.
6. Chambers, A. and Baker, R.T.K., *J. Catal.*, 1996, vol. 158, no. 1, p. 356.
7. Chambers, A., Rodriguez, N.M., and Baker, R.T.K., *J. Mater. Res.*, 1996, vol. 11, no. 2, p. 430.
8. Bernardo, C.A., Alstrup, I., and Rostrup-Nielsen, J.R., *J. Catal.*, 1985, vol. 96, p. 517.
9. Alstrup, I., *J. Catal.*, 1988, vol. 109, p. 241.
10. Van Stiphout, P.C.M., Stoble, D.E., Scheur, F.Th.V.D., and Geus, J.W., *Appl. Catal.*, 1988, vol. 40, p. 219.
11. Chesnokov, V.V., Zaikovskii, V.I., Buyanov, R.A., Molchanov, V.V., and Plyasova, L.M., *Kinet. Katal.*, 1994, vol. 35, no. 1, p. 146.
12. Brotons, V., Coq, B., and Planeix, J.M., *J. Mol. Catal. A: Chem.*, 1997, vol. 116, no. 3, p. 397.
13. Mishakov, I.V., Chesnokov, V.V., Buyanov, R.A., and Pakhomov, N.A., *Kinet. Katal.*, 2001, vol. 42, no. 4, p. 598.